PRAMANA
— journal of
physics

Vol. 59, No. 1
July 2002
pp. 9–18

Critical exponents in the transition to chaos in one-dimensional discrete systems

G AMBIKA and N V SUJATHA
Department of Physics, Maharaja's College, Cochin 682 011, India

MS received 7 June 2001; revised 24 January 2002

Abstract. We report the numerically evaluated critical exponents associated with the scaling of generalized fractal dimensions during the transition from order to chaos. The analysis is carried out in detail in the context of unimodal and bimodal maps representing typical one-dimensional discrete dynamical systems. The behavior of Lyapunov exponents (LE) in the cross over region is also studied for a complete characterization.

Keywords. Critical exponents; Lyapunov exponent; fractal dimensions; period doubling; bimodal maps.

PACS Nos 05.45.+b; 05.40.+j

1. Introduction

The transition from periodic to chaotic behavior in one-dimensional discrete dynamical systems occurs as a function of the external control parameter and is most often characterized by the occurrence of critical exponents. These exponents are associated with the order parameters of the transition. If the transition is via the period doubling route, the Lyapunov exponent (LE) which is a measure of the average divergence rate of two nearby points serves as an effective order parameter. During the onset of chaos that occurs at the accumulation point, the value of LE crosses zero from the negative side to the positive side. Hence the irregular and unpredictable behavior associated with chaos is in particular quantified through LE. As such $1/\lambda$ is a measure of the time correlation in the system. The scaling behavior of λ has been analyzed theoretically and numerically [1] and is found to obey the relation

$$\lambda \approx |\mu - \mu_\infty|^\nu \tag{1}$$

where μ_∞ is the value of the control parameter μ at the Feigenbaum point or accumulation point of period doubling transitions and ν is the associated critical exponent. In the context of unimodal maps like the logistic map, ν is given by the Huberman–Rudnick (HR) relation

$$\nu(z) = \frac{\ln 2}{\ln \delta(z)} \tag{2}$$

where δ is the universal index and z the order of the maximum of the map function characterizing the dynamics of the discrete system. However, near the intermittency prior to a tangent bifurcation the order parameter is the period length $L(\mu)$ [2] which scales as

$$L(\mu) \approx |\mu - \mu_t|^{\zeta} \quad \text{and} \quad \zeta = \frac{1}{z} - 1. \tag{3}$$

So also near transient chaotic behavior like crisis, the scaling is analyzed for the escape rate K with a similar relation

$$K \approx |\mu - \mu_c|^{\eta}. \tag{4}$$

In this work, we consider the possibility of more scaling relations that are relevant in characterizing the geometry of the Cantor set-like attractor [3] near the transition point. The generalized fractal dimensions D_q, when evaluated in the region from μ_∞ to the band merging crisis point μ_b, are found to obey general relations of the type

$$D_q - D_{q_\infty} \approx |\mu - \mu_\infty|^{\theta_q}. \tag{5}$$

For each q, D_{q_∞} is the value of D_q at $\mu = \mu_\infty$ and θ_q is the associated critical exponent. Our calculations show that for q values in the range from -10 to 10, each D_q has three characteristic regions of differing exponents, viz., $\theta_{q_1}, \theta_{q_2}$ and θ_{q_3}, that corresponds to band merging windows of different orders. We present the values of these three exponents and their variations with q for the logistic map and a bimodal cubic map.

The scaling behavior of LE is also analyzed in detail. We find that for the logistic map, the HR relation is true for the overlap scaling while the exponent ν in the immediate neighborhood of μ_∞ is ≈ 1. This is in conformity with the values reported for combination maps [4] and continuous systems [5]. Novel features regarding distributions of λ in regions close to crisis and transition to strange but non-chaotic attractors (SNCA) have been reported earlier [6–8]. For band merging crisis and SNCA to chaos again, linear scaling relations are valid for λ [9,10]. However, bimodal maps considered here exhibit an intermediate region where due to critical slowing down [11], δ in the HR relation (2) is replaced by $\delta^{1/2}$.

The paper is organized as follows: In §2, we introduce the salient features of the unimodal and bimodal maps. In §3, the exponents of the fractal dimensions and their characteristic behavior are reported. The scaling of LE for the two typical cases under study are briefly given in §4 and our concluding remarks are included in the last section.

2. Unimodal and bimodal maps

In this section, we concentrate mainly on continuous maps that are unimodal or bimodal in nature. For unimodal maps, which is modeled most often by the logistic map

$$X_{n+1} = f(X_n, \mu) = \mu X_n (1 - X_n). \tag{6}$$

$f(X_n, \mu)$ has a single critical point $X_c = \frac{1}{2}$ in the defining interval and the function is monotonically increasing for $X < X_c$ and decreasing for $X > X_c$ so that it belongs to the $(+,-)$ group of maps. The transition point μ_∞ is reached via the period doubling scenario and

is characterized mainly by the index δ. The iterates of the map at μ_∞ fall on an inhomogeneous attractor which has the structure of a non-uniform Cantor set and hence demands detailed multifractal analysis in terms of $(D_q - q)$ or $(f - \alpha)$ for the complete resolution of its geometry. The structure of the attractor undergoes continuous and small changes as μ increases from μ_∞. However, before reaching μ_b, there are band merging points of higher orders where the attractor undergoes sudden changes in its pattern. Figure 1 shows these changes in the structure of the attractor from μ_∞, where a 2^∞ attractor exists to the band merging crisis point μ_b, at which a single band is formed. The fractal sets are plotted using 10^4 iterates for a random initial value in [0,1] after discarding the first 3000 iterates, for typical values of μ viz. (a) $\mu_\infty = 3.5699456$, (b) 3.573444, (c) 3.596643 and (d) $\mu_b = 3.675643$. Figure 1b is a zoomed version of a small window in figure 1a. The band merging point can be calculated analytically from the relation [12]

$$f^2(X_c, \mu_b) = \frac{1}{\mu_b}. \tag{7}$$

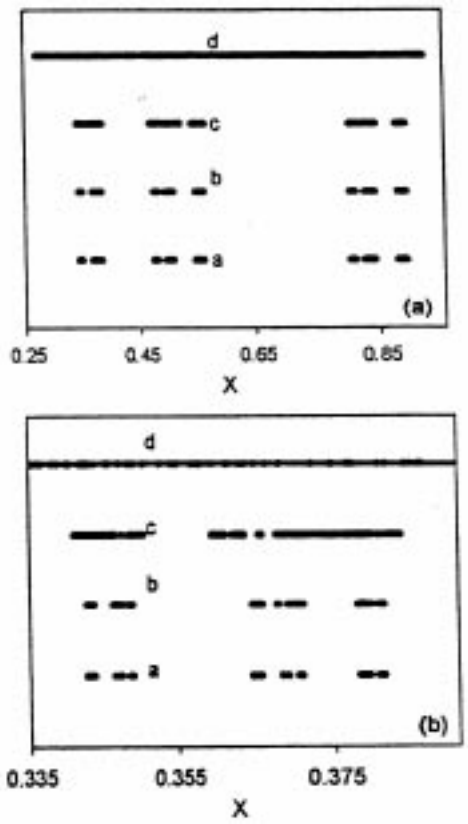

Figure 1. (**a**) The Cantor set structure of the attractor for logistic map using 10^4 iterates, for typical values of μ viz. (a) for $\mu_\infty = 3.5699456$, (b) for 3.573444, (c) for 3.596643 and (d) for $\mu_b = 3.675643$. (**b**) is a zoomed version of a small window in (**a**).

Bimodal maps typically are maps with two critical points X_{c_1} and X_{c_2} with a point of inflection X_i. The simplest among them are cubic maps of the type

$$X_{n+1} = f(X_n, \beta, \mu) = X_n^3 - \beta X_n + \mu. \tag{8}$$

Here the parameter β controls the non-linearity term and μ is an additive parameter, which controls the dynamics of the system. Generally bimodal maps model systems involving coupled oscillators, degree one circle maps and modulated systems [13,14]. In the present form in (8) they have $X_{c_1} = -\sqrt{\beta/3}$ and $X_{c_2} = +\sqrt{\beta/3}$ and the inflection point is at $X_i = 0$. The map function is monotonically increasing for $X < X_{c_1}$, decreasing for $X_{c_1} < X < X_{c_2}$ and increasing for $X > X_{c_2}$ so that it belongs to (+-+) type of bimodal map. The derivative function $f' = \mathrm{d}f/\mathrm{d}x$ is piecewise monotonic and continuous with a single critical point which is a minimum at $X = X_i$. The stability and the asymptotic states of (8) mainly depends on the behavior of f' especially near its inflection point. Since f' is concave in shape, f''' at $X = X_i$ is greater than zero. For a given value of the parameter β, as μ is varied, the cycle elements from a period doubling bifurcation have a tendency to merge together to form a closed loop or bubble-like structure finally ending in the 1-cycle [15,16]. Here studies based on RG analysis by Oppo and Politi [11] have revealed a critical slowing down near the Feigenbaum point, where chaos just disappears. In our numerical analysis, this has been explicitly verified by fixing the multiplicative parameter β at the limiting point $\beta_\infty = 1.742821997236$....and varying μ until the chaotic region disappears at $\mu = \mu_\infty$. The bifurcation values show a rate $\delta^{1/2}$ and the gradual increase of β from β_∞ reveals the growth of the convergence rate from $\delta^{1/2}$ to δ as the number of bifurcations $\to\infty$.

3. Scaling behavior in fractal dimensions

The geometry of the chaotic attractor is resolved through the generalized dimensions D_q or equivalently the $(f-\alpha)$ spectrum [17]. In this work we concentrate on the dimensions D_q, for q values ranging from -10 to $+10$. Thus a complete characterization of the small scale variations of the non-uniformities in the fractal set is feasible. As μ is increased beyond μ_∞, the intervals start merging and hence the values of D_q also changes in a particular pattern, which can be captured in the scaling of D_q as a function of μ. This is the motivation for studying scaling behavior and evaluating critical exponents, that can reveal typical patterns of behavior at the secondary level, the primary level being the values of (D_q, q). If we consider the reverse sequence from μ_b to μ_∞, a single band splits into twice as many bands following ideally the steps in the construction of a Cantor set and reaching an infinite number of points of zero length at μ_∞. The band merging takes place in the forward direction; the merging of order 2^n to 2^{n-1} $(n = 1, 2, 3, \ldots)$ takes place when the unstable fixed points created during the bifurcation of 2^{n-1} cycle to 2^n hits the band of order 2^n.

The values of D_q in the parameter range of interest viz. μ_∞ to μ_b are calculated numerically using their defining relations [18]. The variation of D_q with the parameter for $q = 0, 1, 2$ is given in figure 2 for the logistic and bimodal cubic maps. The critical exponents are evaluated from the plot of $\log|D_q - D_{q_\infty}|$ vs. $\log|\mu - \mu_\infty|$, that are also shown in the same figure. It is clear that there are three prominent scaling regions giving three different slopes viz. $\theta_{q_1}, \theta_{q_2}$ and θ_{q_3} for each q value. By checking the parameter values at which the change from one scaling region to another takes place, with the higher order

band merging points, we come to the following conclusion. For mergings from 2^{∞} bands to 2^3 bands, almost the same exponent θ_{q_1} is obtained, reflecting a more or less average behavior in the pattern of changes in the corresponding Cantor set. However, prior to the region where 2^3 to 2^1 and 2^1 to 2^0, there are major changes in structure giving differing values for the exponents θ_{q_2} and θ_{q_3} respectively. The values of these exponents for the two cases under study for $q = 0, 1, 2$ are given in table 1.

In figure 3, we study the variation of these three exponents with q for the logistic map. The variations are fitted with a six degree polynomial whose expressions are

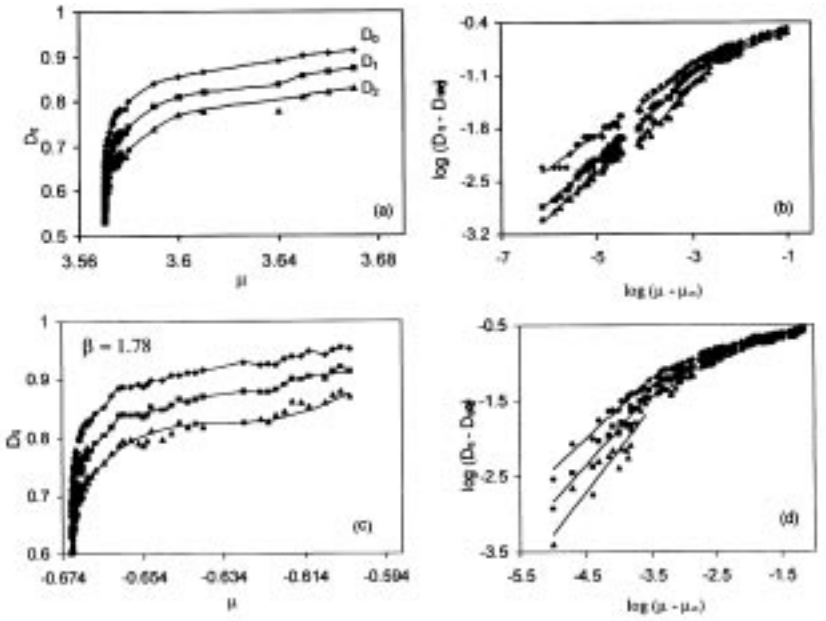

Figure 2. The variations of the dimensions D_q for $q = 0, 1$ and 2 with the parameter μ. (**a**) for logistic map and (**c**) for bimodal cubic map, from the Feigenbaum point μ_∞ to the band merging crisis point μ_b. (**b**) and (**d**) show the corresponding logarithmic plots of $(D_q - D_{q_\infty})$ vs. $(|\mu - \mu_\infty|)$. The critical exponents θ_q are evaluated as the slopes of the above plots. The three regions of differing θ_q's for each D_q are clearly evident.

Table 1. The scaling indices in three different regions calculated from the plots in figure 2.

		Scaling indices for		
Map function	θ	D_0	D_1	D_2
Logistic	θ_{q_1}	0.3866	0.4501	0.5510
	θ_{q_2}	0.2865	0.3785	0.3552
	θ_{q_3}	0.1765	0.2199	0.2454
Bimodal cubic	θ_{q_1}	0.5877	0.7291	0.8436
	θ_{q_2}	0.1994	0.2020	0.2340
	θ_{q_3}	0.1536	0.1491	0.1344

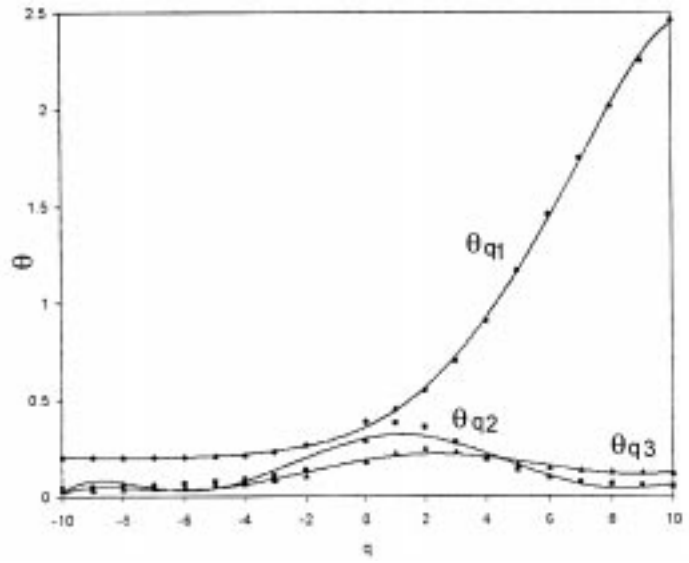

Figure 3. The variations of the three exponents $\theta_{q_1}, \theta_{q_2}$ and θ_{q_3} with q for $q = -10$ to $+10$ for the logistic map. The curves can be fitted with a six degree polynomial whose equations are given in the text.

$$\theta_{q_1} = -(3E-07)q^6 - (7E-06)q^5 - 6(E-06)q^4 + 0.001q^3 + 0.014q^2 + 0.072q + 0.36 \quad (9)$$

$$\theta_{q_2} = -(9E-07)q^6 + 6(E-06)q^5 + (2E-04)q^4 - (9E-04)q^3 - 0.012q^2 + 0.03q + 0.3 \quad (10)$$

$$\theta_{q_3} = -(3E-07)q^6 + (3E-06)q^5 + (6E-05)q^4 - (6E-04)q^3 - 0.004q^2 + 0.026q + 0.19. \quad (11)$$

The curves are almost horizontal for negative q values and changes considerably for $q > 0$. θ_{q_1} shows an almost monotonic increase while θ_{q_2} and θ_{q_3} increases to reach a maximum and then decreases. The analysis is repeated for the bimodal map by keepng $\beta = 1.78$ and evaluating the corresponding μ_∞ as -0.6717398814998050 and μ_b as -0.6327445. The results are furnished in figure 4 and the polynomial fits of degree six are

$$\theta_{q_1} = -(2E-07)q^6 + (E-05)q^5 + (4E-05)q^4 - 0.002q^3 - 0.002q^2 + 0.134q + 0.575 \quad (12)$$

$$\theta_{q_2} = -(7E-08)q^6 + (E-06)q^5 + (2E-05)q^4 - (2E-04)q^3 - 0.002q^2 + 0.02q + 0.197 \quad (13)$$

$$\theta_{q_3} = -(4E-07)q^6 + (E-06)q^5 + (8E-05)q^4 - (2E-04)q^3 - 0.005q^2 + 0.006q + 0.139. \quad (14)$$

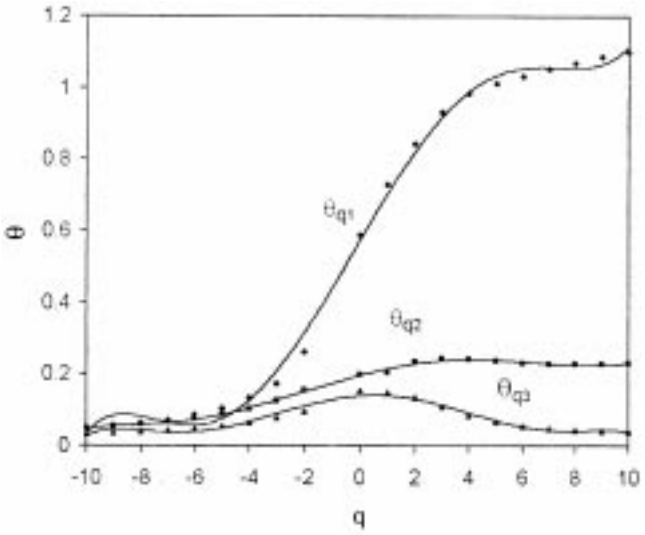

Figure 4. The variations of θ_{q_1}, θ_{q_2} and θ_{q_3} with q values for the bimodal cubic map.

4. Scaling of Lyapunov exponents

The scaling behavior of LE for unimodal maps generally follow the HR relation (2). This has been verified for a large class of maps with different z values [4]. However, it is well-known that this relation was derived based on the mirror symmetric band merging or splitting on the chaotic side beyond μ_∞. Other approaches of this behavior are done in the presence of noise, the limit of the noise amplitude $\to 0$ reproducing (2) [19]. Obviously this has the effect of washing out of all periodic windows and hence corresponds to overlap scaling. Numerical results available in the literature [20] are mostly overlap scaling and thus seems to avoid the critical region in the immediate neighborhood of μ_∞. We mainly focus on this region and work out the index ν for logistic and bimodal cubic map. Figure 5 gives the results of our calculations for the logistic map in the region near μ_∞ and the overlap region is also included for comparison. The log–log plots give slope $\nu = 1.0008$ in the former case and the HR value of 0.4474 in the latter case. We do the analysis numerically for the bimodal map also in the immediate neighborhood of μ_∞. The Feigenbaum point is calculated using numerical search procedure with an accuracy up to 10^{-10}–10^{-12}. Then we fix the β value at $\beta = 1.743$ and find out the corresponding μ_∞ as $-0.489564892649939...$ at which $\lambda \approx 8.43 \times 10^{-10}$. μ is then changed in steps of the order say 10^{-12} to 10^{-6} and the corresponding LE's computed numerically. Figures 6a, 6c and 6e show the variation of LE with the parameter μ. The critical exponent ν is calculated as the average slope of the log–log plot between λ and $|(\mu - \mu_\infty)|$. Figures 6b, 6d and 6f show the three regions of differing ν values; figure 6b for linear scaling 6d for an intermediate region where critical slowing down prevails and 6f for overlap scaling. The above analysis is repeated for different β values and the results are condensed in table 2.

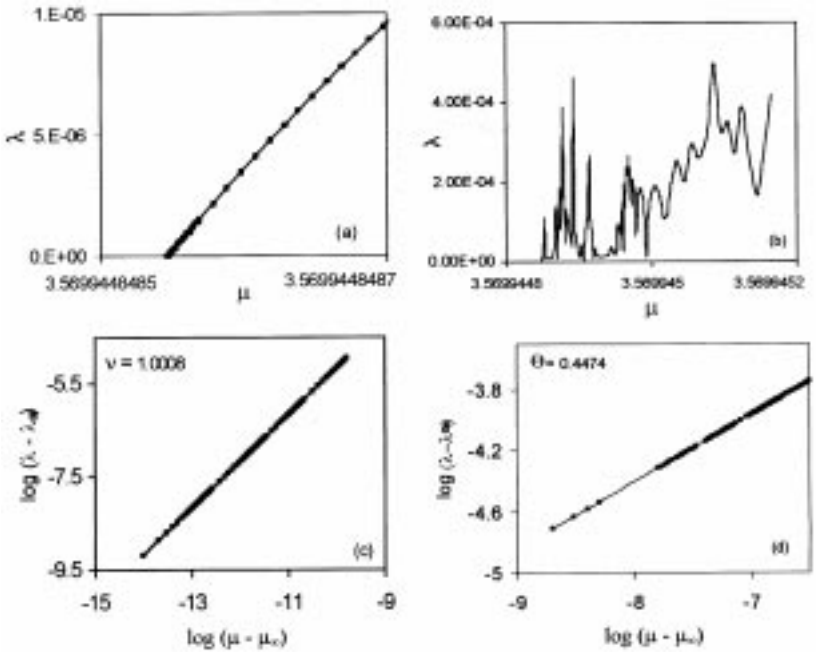

Figure 5. The behavior of the LE, λ, of the logistic map with the control parameter μ. (**a**) in the immediate neighborhood of μ_∞ where the behavior is linear with $\nu \approx 1$, (**c**) for the region of overlap scaling, where $\nu \approx \ln 2/\ln \delta \approx 0.4474...$ (**b**) and (**d**) are the corresponding logarithmic plots of λ vs. $(|\mu - \mu_\infty)|$. The scaling index ν is the slope of the log–log plot.

Table 2. The critical points μ_∞, λ at μ_∞ and the corresponding scaling indices for different β values for the bimodal map.

β	μ_∞	λ at μ_∞	ν
1.743	-0.4895648926499390	$8.43E-10$	1.003418
1.75	-0.5603536900309620	$1.74E-10$	1.000035
1.765	-0.6245698878069280	$3.60E-12$	1.000131
1.78	-0.6717398814998050	$3.68E-12$	1.000769

5. Conclusion

In this study, we work with two typical maps or discrete dynamical systems viz. the logistic map and a bimodal cubic map, in their transition regions from order to chaos characterized by the parameter value μ_∞. The generalized fractal dimensions characterizing the geometry of the attractor in general have three prominent scaling regions and the variation of the corresponding exponents θ_q with q follow polynomial relations. The order parameter

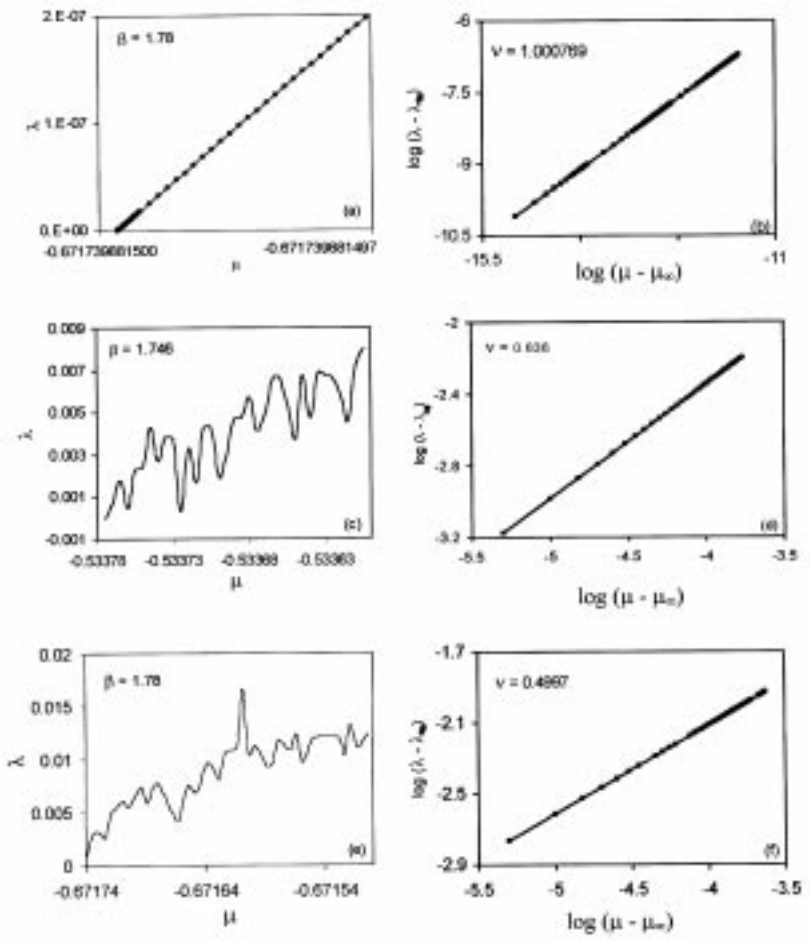

Figure 6. The variation of λ with μ for bimodal cubic map (**a**) in the immediate neighborhood of μ_∞ where $\nu \approx 1$, (**c**) for the intermediate region of critical slowing down and (**e**) for regions of overlap scaling. (**b**), (**d**) and (**f**) are the corresponding log–log plots of λ vs. $(|\mu - \mu_\infty)|$.

characterizing the dynamics on the attractor viz. the Lyapunov exponent shows linear scaling with an exponent $\nu \approx 1$ in the immediate neighborhood of μ_∞. The novel feature of the work reported here is the addition of critical exponents θ_q, which reflects the pattern of changes in the fractal structure of the Feigenbaum attractor as the parameter changes. However in the context of bimodal maps, this structure should depend on the specific route or kneading sequence that the system follows to reach the Feigenbaum point. In the present work, we concentrate only on the period doubling route. For other combinations of parameter values, several other kneading sequences are possible [21]. The search for scaling in the analogous approach with $(f - \alpha)$ values is being done and will be reported elsewhere.

Acknowledgements

NVS acknowledges the University Grants Commission, New Delhi for assistance through Junior Research Fellowship and GA acknowledges the computer facility and warm hospitality at IUCAA, Pune.

References

[1] B A Huberman and J Rudnick, *Phys. Rev. Lett.* **45**, 154 (1980)
[2] C Beck and F Schlogl, *Thermodynamics of chaotic systems* (Cambridge University Press, 1993)
[3] Ali H Nayfeh and B Balachandran, *Applied nonlinear dynamics* (Wiley-Interscience Pub, 1995)
[4] P R Krishnan Nair, V M Nandakumaran and G Ambika, *Pramana – J. Phys.* **43**, 421 (1994)
[5] G Ambika, *Phys. Lett.* **A221**, 323 (1996)
[6] V Mehra and R Ramaswamy, *Phys. Rev.* **E53**, 3420 (1996)
[7] A Prasad, V Mehra and R Ramaswamy, *Phys. Rev. Lett.* **79**, 4127 (1997)
[8] A Prasad, V Mehra and R Ramaswamy, *Phys. Rev.* **E57**, 1576 (1998)
[9] Y C Lai, *Phys. Rev.* **E53**, 57 (1996)
[10] P Philominathan and P Neelamegham, *Chaos, solitons and fractals* **12**, 1005 (2001)
[11] G L Oppo and A Politi, *Phys. Rev.* **A30**, 435 (1984)
[12] N Ananthkrishnan and Tuhin Sahai, *Resonance* **6**, No. 3, 19 (2001)
[13] T Hogg and B A Huberman, *Phys. Rev.* **A29**, 275 (1984)
[14] J Kozlowski, U Parlitz and W Lauterborn, *Phys. Rev.* **E51**, 1861 (1995)
[15] G Ambika and N V Sujatha, *Pramana – J. Phys.* **54**, 751 (2000)
[16] G Ambika, N V Sujatha and K P Harikrishnan, *Proceedings of VIIIth Ramanujam symposium on recent developments in nonlinear systems held on Feb. 14–16, 2001* (in press)
[17] G Ambika and K Babu Joseph, *Pramana – J. Phys.* **39**, 193 (1992)
[18] R C Hilborn, *Chaos and nonlinear dynamics* (Oxford University Press, 1994)
[19] B Shraiman, C E Wayne and P C Martin, *Phys. Rev. Lett.* **46**, 935 (1981)
[20] J Crutchfield, M Nauenberg and J Rudnick, *Phys. Rev. Lett.* **46**, 933 (1981)
[21] K F Cao and S L Peng, *Phys. Rev.* **E60**, 2745 (1999)